Catalytic combustion of methane in simulated PSA offgas over Mn-substituted La–Sr-hexaaluminate (La$_x$Sr$_{1-x}$MnAl$_{11}$O$_{19}$)

Seongmin Kim [a], Dae-Won Lee [b,**], Joon Yeob Lee [a], Hee-Jun Eom [a], Hwa Jung Lee [a], In-ho Cho [c], Kwan-Young Lee [a,*]

[a] Department of Chemical & Biological Engineering, Korea University, Anam-dong, Seongbuk-gu, Seoul 136-713, Republic of Korea
[b] Research Institute of Clean Chemical Engineering Systems, Korea University, Anam-dong, Seongbuk-gu, Seoul 136-713, Republic of Korea
[c] Corporate R&D Center, SK Energy, Daejeon 305-712, Republic of Korea

ABSTRACT

Mn-substituted La, Sr-hexaaluminate was studied as a catalyst for the catalytic combustion of pressure swing adsorption (PSA) offgas from a hydrogen station based on steam reforming of petroleum gas. The catalytic activity and thermal stability were tested under simulated PSA offgas condition and the catalysts were characterized by X-ray diffraction (XRD), inductively coupled plasma atomic emission spectroscopy (ICP-AES), CO$_2$-temperature programmed desorption (TPD) and N$_2$ physisorption for BET. All the La$_x$Sr$_{1-x}$MnAl$_{11}$O$_{19}$ catalysts prepared by co-precipitation method contained hexaaluminate structure as the major phase after 5 h calcination at 1200 °C. Partial substitution of La for Sr in SrMnAl$_{11}$O$_{19}$ increased the specific surface area and consequently the catalytic activity for oxidation of methane. The CO$_2$ in the simulated PSA offgas was found to suppress the catalytic activity in methane oxidation if the catalyst had appreciable surface basicity. The most active catalyst, La$_{0.6}$Sr$_{0.4}$MnAl$_{11}$O$_{19}$, retained its lattice structure and chemical composition even after 40-h thermal aging at 1000 °C under PSA offgas composition.

© 2010 Elsevier B.V. All rights reserved.

1. Introduction

As a heat source for various chemical processes, a conventional flame combustion has several problems such as emission of NOx and unburned hydrocarbons, as well as low energy efficiency [1]. As an alternative, catalytic combustion has been widely researched over the last few decades due to its superior efficiency and low emission of pollutants [2–5]. In catalytic combustion processes, however, the durability is the issue, because hot spots or temperature runaway occasionally occur in the catalyst, which seriously deactivates the catalysts. Therefore, thermal stability is an important factor for developing combustion catalysts.

Noble metals such as Pt and Pd have been suggested as the most promising catalysts for catalytic combustion. However, the loss of active surface sites through thermal aggregation or volatilization is a drawback against high temperature application, in addition to the disadvantage of high material cost. Therefore, metal oxide catalysts have attracted attention as an alternative to noble metal catalysts due to their decent thermal stability and relatively low preparation cost. Ceria, zirconia, ceria-zirconia, perovskite and hexaaluminate have been studied for catalytic combustion of methane [6–15]. Hexaaluminate is a promising catalytic material due to its outstanding thermal stability and reasonable oxidation activity. Arai and Machida proposed hexaaluminate as a catalytic material for the high-temperature catalytic combustion of methane [11,13,14]. In the general hexaaluminate formula of AB$_x$Al$_{12-x}$O$_{19}$, A-site is mainly an alkaline, alkaline-earth or rare-earth metal, and B-site a transition metal such as Cr, Ni, Co, Fe or Mn, having a similar radius to Al. It was reported that the hexaaluminate catalyst with Mn as the B-site atom is especially good for catalytic combustion of methane [13]. In this case, the redox cycle between Mn^{2+} and Mn^{3+} is regarded as the main source of the combustion activity [15].

Recently, much researches and developments have focused on hydrogen stations as the major infrastructure for the upcoming "Hydrogen Economy". In a hydrogen station, pressure swing adsorption (PSA) unit has been widely adopted as a final separation tool to obtain high purity hydrogen. The waste effluent derived from PSA unit, which is usually labeled as PSA offgas, can be utilized as a fuel for catalytic combustor supplying heat to the steam reformer with a purpose of improving energy efficiency of the overall process [16]. When petroleum gas is used as the hydrogen source for steam reformer, PSA offgas at the tail of the process usually contains CH$_4$, CO, CO$_2$, H$_2$ and H$_2$O, of which CH$_4$, CO and H$_2$ are combustible. Although H$_2$ is abundant and has the highest heating

value (119.96 MJ/kg) among them, oxidation of CH_4 is more significant because CH_4 is the most difficult to oxidize and requires high temperature for its oxidation, whereas CO and H_2 are likely to incinerate at low temperature. In addition, as CH_4 is 23 times more effective than CO_2 as a greenhouse gas [17], its emission should be reduced as much as possible. Therefore, CH_4 conversion should be chosen as the measure for the performance of a combustion catalyst when the PSA offgas is used as a fuel.

So far, hexaaluminate has been mostly studied for the catalytic combustion of gasified biomass and its thermal stability has been proved in the literature [18]. However, it has not yet been studied for the catalytic combustion of PSA offgas. In this study, the combustion activity and thermal stability of $La_xSr_{1-x}MnAl_{11}O_{19}$ were investigated under simulated PSA offgas conditions.

2. Experimental

$La_xSr_{1-x}MnAl_{11}O_{19}$ ($x = 0-1$) was prepared via co-precipitation method. Stoichiometric amounts of $La(NO_3)_3 \cdot xH_2O$, $Sr(NO_3)_2$, $Mn(NO_3)_2 \cdot 4H_2O$ and $Al(NO_3)_2 \cdot 9H_2O$ (Aldrich) were dissolved in de-ionized water, separately. Precursor solutions of La, Sr and Mn were poured into the aluminum nitrate solution at 60 °C. Ammonium carbonate solution was added until the pH of the solution reached 7–8. The solution was aged for 5 h at 60 °C under vigorous stirring, and then the precipitate was filtered and washed with de-ionized water. The filtered cake was dried at 110 °C overnight and calcined at 1200 °C for 5 h in air condition.

The crystalline structures of the samples were analyzed by X-ray diffraction (D/MAX-IIIB X-Ray Diffractometer, Rigaku) using Cu Kα radiation. The specific surface area was measured by the BET method using N_2 adsorption at 77 K (ASAP2010, Micromerics). The elemental composition was analyzed by ICP-AES (138 Ultrace, Jobin-Yvon). The basicity of a catalyst was analyzed through CO_2-temperature programmed desorption experiment (BELCAT-M-77, BEL Japan Inc.). 0.1 g of sample was pretreated under 40 ml/min of He at 950 °C for 1 h and CO_2 adsorption was performed under 40 ml/min of pure CO_2 at 100 °C for 1 h. Then, the CO_2 desorption profile was recorded with raising the temperature from 50 °C to 800 °C at the rate of 20 °C/min under 40 ml/min of He.

The reaction tests were performed using a flow-type packed bed reactor. Methane combustion was evaluated under two conditions: a methane–oxygen gas mixture of 1 vol% CH_4 and 20 vol% O_2, and a simulated PSA offgas of 1 vol% CH_4, 6 vol% H_2, 0.7 vol% CO, 7.5 vol% CO_2, 0.2 vol% H_2O and 20 vol% O_2, which simulated the offgas composition from the hydrogen station demonstrated by SK energy at Daejeon, South Korea. The total flow rate was 500 ml/min with balanced N_2 and the weight of catalyst was 0.5 g. The temperature at the center of catalyst bed was controlled as the reaction temperature. Moisture in the gas flow was removed by cold trap and the gas composition was analyzed through gas chromatography (Acme 6000, Younglin) equipped with a packed column, Carbosieve SII (Supelco).

Thermal aging tests were performed under simulated PSA offgas condition. Catalysts were aged at 1000 °C for 40 h. The catalytic activity was measured every 10 h under PSA offgas but the reaction temperature was set to 650 °C, because at high temperature of 1000 °C, where the aging was performed, the differences of combustion activity among catalysts could be indistinguishable.

3. Results and discussion

3.1. Crystal structure

The XRD patterns of the prepared hexaaluminates are shown in Fig. 1. All the catalysts prepared by co-precipitation method
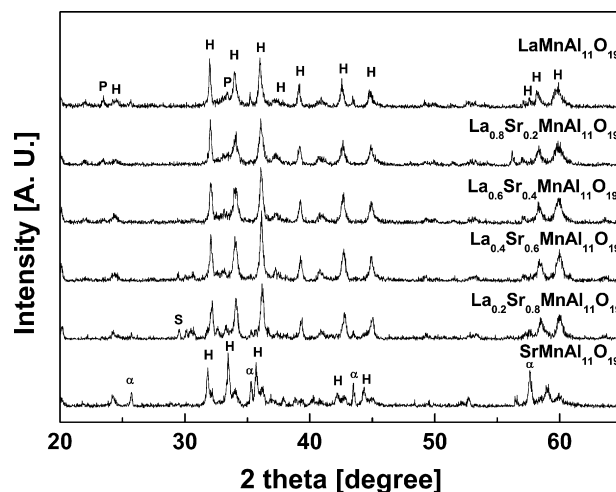

Fig. 1. XRD patterns of $La_xSr_{1-x}MnAl_{11}O_{19}$ ($x = 0, 0.2, 0.4, 0.6, 0.8, 1$). H: hexaaluminate; P: $LaAlO_3$; α: α-Al_2O_3; S: $SrAl_2O_4$.

exhibited a predominance of hexaaluminate after calcination at 1200 °C for 5 h. Small amounts of α-Al_2O_3 (JCPDS #46-1212) and $LaAlO_3$ (JCPDS #31-0022) were observed in the patterns. About the presence of $LaAlO_3$, Zheng et al. explained that $LaAlO_3$ was formed through the solid state reaction between La_2CO_3 and Al_2O_3 [19]. Especially, the structures of $La_{0.6}Sr_{0.4}MnAl_{11}O_{19}$ and $La_{0.8}Sr_{0.2}MnAl_{11}O_{19}$ were nearly pure hexaaluminate with comparatively small amounts of impurities such as perovskite, spinel and α-alumina.

3.2. Specific surface area

The specific surface areas of hexaaluminates are listed in Table 1. With increasing the content of La, the specific surface areas of $La_xSr_{1-x}MnAl_{11}O_{19}$ increased and reached maximums of 23 and 25 m^2/g at $x = 0.6$ and 0.8, respectively. The specific surface area of hexaaluminate is related to the mirror plane located in the lattice [11,14]. This mirror plane is positioned vertically on the c-axis of the unit cell, thereby separating the layers, restricting the crystal growth of the structure along the c-axis and stabilizing the structure at high temperature [14]. A-site metal cations are located in the mirror plane, so that the La/Sr ratio at A-site affects the lattice dimension and crystal size [14,20]. These variations were considered to affect the surface area of $La_xSr_{1-x}MnAl_{11}O_{19}$.

3.3. Catalytic activity

Fig. 2 and Table 1 show the results of the methane oxidation over $La_xSr_{1-x}MnAl_{11}O_{19}$ under methane–oxygen gas mixture. The temperature when the methane conversion reaches x% is designated as $T_{x\%}$ at Table 1. With the largest BET areas, $La_{0.8}Sr_{0.2}MnAl_{11}O_{19}$

Table 1
Summary of specific surface area and catalytic activity expressed as $T_{10\%}$ and $T_{90\%}$ of catalysts ($T_{10\%}$ and $T_{90\%}$ were approximated from the reaction results displayed in Fig. 2).

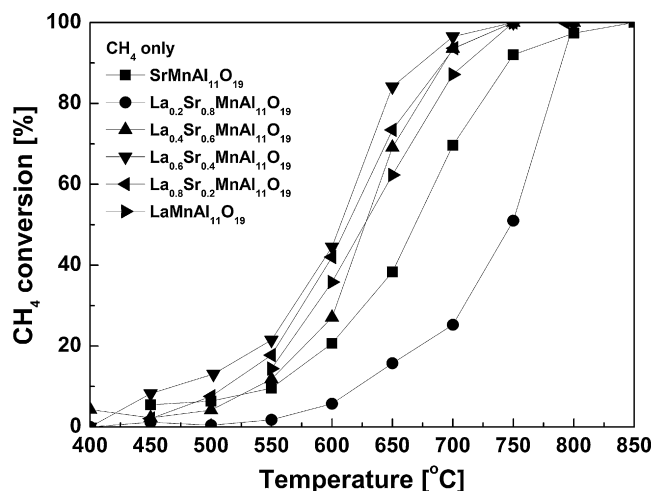| Catalyst	Surface area (m^2/g)	Methane–oxygen mixture (°C)	
		$T_{10\%}$	$T_{90\%}$
$LaMnAl_{11}O_{19}$	13	<550	710
$SrMnAl_{11}O_{19}$	9	550	745
$La_{0.8}Sr_{0.2}MnAl_{11}O_{19}$	25	510	680
$La_{0.6}Sr_{0.4}MnAl_{11}O_{19}$	23	470	675
$La_{0.4}Sr_{0.6}MnAl_{11}O_{19}$	16	540	690
$La_{0.2}Sr_{0.8}MnAl_{11}O_{19}$	3	620	790

Fig. 2. Catalytic combustion of methane over $La_xSr_{1-x}MnAl_{11}O_{19}$ ($x = 0, 0.2, 0.4, 0.6, 0.8, 1$) under methane (1%)–oxygen (20%) mixture.

Fig. 4. Catalytic combustion of methane over $La_xSr_{1-x}MnAl_{11}O_{19}$ ($x = 0, 0.2, 0.4, 0.6, 0.8, 1$) under simulated PSA offgas.

and $La_{0.6}Sr_{0.4}MnAl_{11}O_{19}$ showed the best activities (the lowest $T_{10\%}$) among the tested hexaaluminate catalysts, whereas $La_{0.2}Sr_{0.8}MnAl_{11}O_{19}$ and $SrMnAl_{11}O_{19}$, which possessed the lowest BET surface areas, showed the lowest methane conversions. Hence, we concluded that the activity of methane oxidation over $La_xSr_{1-x}MnAl_{11}O_{19}$ at methane–oxygen mixture was generally dependent on the specific surface area of the catalyst. This result is similar to that of Li et al. who correlated the combustion activity of hexaaluminate with its surface area [21]. The redox cycle of $Mn^{2+} \leftrightarrow Mn^{3+}$ in B-site is the main element of the oxidation mechanism over Mn-substituted hexaaluminate and mixing La and Sr as A-site metal affects the redox rate of Mn. Li and Wang explained that mixing La^{3+} (radius = 0.106 nm) with larger cation like Ba^{2+} (0.134 nm) in A-site affects the thickness of mirror plane by distorting the lattice structure and expected that the lattice oxygens located on the thicker mirror plane become more mobile, which would lead to higher oxidation activity [20]. Mixing La^{3+} with Sr^{2+} is expected to show similar effects because the ionic radius of Sr^{2+} is also bigger (0.120 nm) than that of La^{3+}. When La–Sr mixed catalysts ($La_xSr_{1-x}MnAl_{11}O_{19}$) were compared with La–Ba ones ($La_xBa_{1-x}MnAl_{11}O_{19}$) about methane oxidation activity, the former were superior to the latter, as clearly seen in Fig. 3. Therefore, the

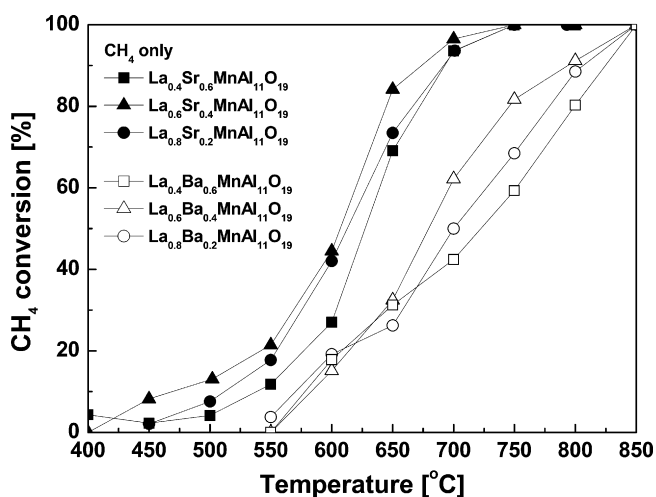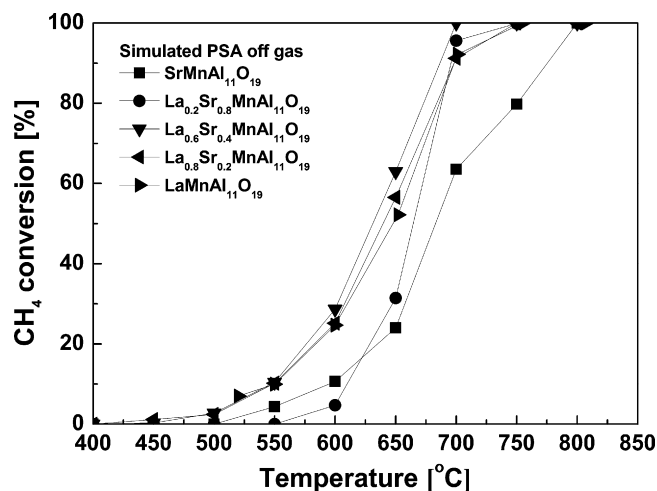increases of surface area and improved redox property were considered to be the main reasons for the enhanced oxidation activity accompanied by mixing La and Sr as A-site atom.

The catalytic combustion of methane at simulated PSA off gas is presented in Fig. 4. The results exhibited a similar tendency to that of methane oxidation activity obtained previously under the methane–oxygen gas mixture. $La_xSr_{1-x}MnAl_{11}O_{19}$ ($x = 0.6$ and 0.8) showed the lowest ignition temperature ($T_{10} \approx 550\,^\circ C$), whereas La–Sr-hexaaluminate at low La content of $x = 0$ and 0.2 showed the highest ignition temperature ($T_{10} > 600\,^\circ C$).

Comparing the result (Fig. 4) with the previous one (Fig. 3), methane conversion of $La_xSr_{1-x}MnAl_{11}O_{19}$ ($x = 0, 0.6, 0.8, 1$) was decreased under the simulated PSA off gas, while, that of $La_{0.2}Sr_{0.8}MnAl_{11}O_{19}$ was increased. Moreover, the use of the simulated PSA off gas reduced the gaps of methane conversion between the catalysts. Each additional gas (CO_2, H_2O, CO and H_2) is expected to make an effect on catalytic activity in an individual way. Cimino et al. stated that the addition of reactive fuel, H_2 and CO, generates additional heat through their oxidation and facilitates the oxidation of methane thermally [22]. Meanwhile, Eriksson et al. stated that CO_2 in the feed influenced oxidation activity and the effect was considerably related to the basicity of catalysts [23].

In order to investigate the relationship between surface basicity and the decrease of oxidation activity for hexaaluminates, the CO_2-TPD experiments were performed (Fig. 5). For La-rich hex-

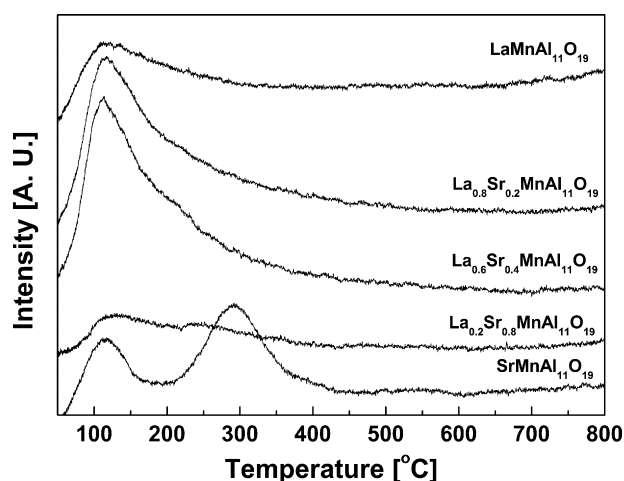**Fig. 3.** Comparison of catalytic methane combustion activities between $La_xSr_{1-x}MnAl_{11}O_{19}$ and $La_xBr_{1-x}MnAl_{11}O_{19}$ ($x = 0.4, 0.6, 0.8$) under methane (1%)–oxygen (20%) mixture.

Fig. 5. CO_2-TPD results of $La_xSr_{1-x}MnAl_{11}O_{19}$ ($x = 0, 0.2, 0.6, 0.8, 1$).
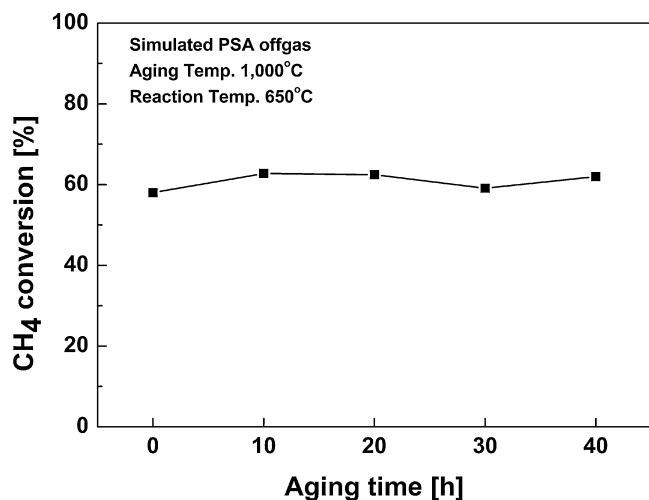
Fig. 6. Methane conversion of $La_{0.6}Sr_{0.4}MnAl_{11}O_{19}$ at 650 °C during the thermal aging test at 1000 °C under simulated PSA offgas.

Fig. 7. XRD patterns of $La_{0.6}Sr_{0.4}MnAl_{11}O_{19}$ before and after thermal aging test. H: hexaaluminate; P: $LaAlO_3$; α: α-Al_2O_3.

Table 2
ICP-AES results of $La_{0.6}Sr_{0.4}MnAl_{11}O_{19}$ before and after thermal aging test.

$La_{0.6}Sr_{0.4}MnAl_{11}O_{19}$	Fresh		After aging 1000 °C, for 40 h		Difference
	ppm	%	ppm	%	%
La	76,500	10.9	75,680	11.4	0.5
Sr	50,420	7.2	47,900	7.2	0.5
Mn	77,470	11.0	72,640	10.9	0.1
Al	499,600	71.0	469,200	70.5	0.5

aaluminates like $La_xSr_{1-x}MnAl_{11}O_{19}$ (x = 0.6, 0.8, 1), they have one broad desorption peak appeared around the temperature range of 50–200 °C. On the other hand, $SrMnAl_{11}O_{19}$ showed additional desorption peak around 300 °C, implying that it has the basic sites stronger than those on the La-rich hexalumi-nates. $La_{0.2}Sr_{0.8}MnAl_{11}O_{19}$, which is Sr-rich in A-site composition, showed the profile similar to $SrMnAl_{11}O_{19}$ but the population of overall basic sites was quite low, which was enough to be classified as a non-basic material.

Correlating these observations with methane oxidation activi-ties, the hexaaluminates having basic sites, $La_xSr_{1-x}MnAl_{11}O_{19}$ (x = 0, 0.6, 0.8, 1), showed the retardation of activities when CO_2 was contained in the reaction mixture, while non-basic $La_{0.2}Sr_{0.8}MnAl_{11}O_{19}$ did not show such negative effect of CO_2 but show the increment of activity as the simulated PSA offgas involved. From these results, a conclusion can be drawn that CO_2 would dete-riorate the oxidation activity of hexaaluminate if the catalyst has an appreciable surface basicity. The increase of activity for non-basic $La_{0.2}Sr_{0.8}MnAl_{11}O_{19}$ is expected to be induced by oxidation of reac-tive fuels (H_2 and CO), as Cimino et al. had explained in their study about methane combustion over perovskite catalyst [22].

3.4. Thermal aging test

A thermal aging test was conducted using $La_{0.6}Sr_{0.4}MnAl_{11}O_{19}$ at 1000 °C. The methane conversion was 58% in the fresh state (Fig. 6 at time = 0), which was slightly lower than the result (63%) of pre-vious activity measurement (Fig. 4). The discrepancy is likely to originate from the differences in the temperature distribution over catalyst bed. The result at 650 °C in Fig. 4 was obtained after passing through the activity measurements at 400–600 °C, while the fresh catalyst of Fig. 6 did not pass through such procedure. Between the two cases, the temperature gradients over catalyst bed could be different even though the temperature in the center of catalyst bed is identically adjusted to 650 °C. The distribution of slightly lower temperature is expected for the catalyst bed at fresh activity test (time = 0) in Fig. 6, resulting in the relatively depressed activity compared with that of Fig. 4.

The XRD results of fresh and aged $La_{0.6}Sr_{0.4}MnAl_{11}O_{19}$ are shown in Fig. 7. There are no indications about the formation of new species or the deformation of hexaaluminate phase after the aging test. As seen in the ICP-AES results in Table 2, the ele-mental concentrations remained also constant after the aging test. These XRD and ICP-AES results confirmed the thermal stability of
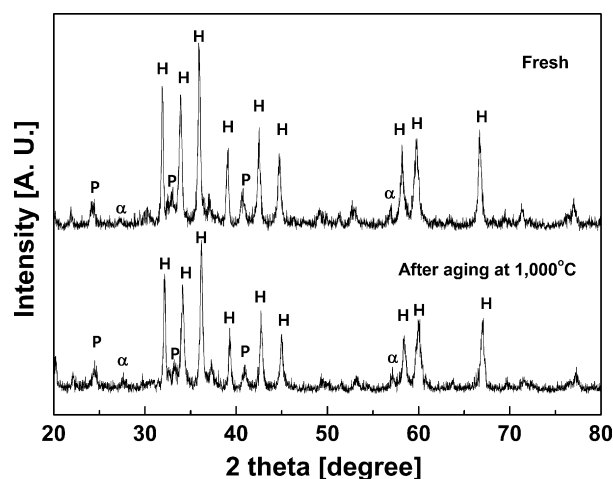
$La_{0.6}Sr_{0.4}MnAl_{11}O_{19}$ during the combustion of PSA offgas.

4. Conclusions

Mn-substituted La–Sr-hexaaluminate ($La_xSr_{1-x}MnAl_{11}O_{19}$, x = 0–1) prepared by co-precipitation method showed a hexaalu-minate structure in major. The mixing of Sr and La in the A-site position was considered to affect the specific surface area and redox property of Mn in Mn-substituted hexaaluminate. The $La_xSr_{1-x}MnAl_{11}O_{19}$ at x = 0.6, 0.8 showed the best combustion activities with the highest specific surface area. When the sim-ulated PSA off gas was used, it was found that high content of CO_2 in the feed stream influenced on the catalytic activity of hexaaluminates having surface basicity. And promoting effect of fuel gases (H_2 and CO) also observed in case of the catalyst having low basicity. Throughout a 40-h thermal aging test at 1000 °C under simulated PSA offgas composition, the activity of $La_{0.6}Sr_{0.4}MnAl_{11}O_{19}$ remained almost constant with no signs of phase deformation and elemental loss.

References

[1] P. Gélin, M. Primet, Appl. Catal. B: Environ. 39 (2002) 1–37.
[2] K. Persson, A. Ersson, K. Jansson, J.L.G. Fierro, S.G. Järås, J. Catal. 243 (2006) 14–24.
[3] J.M. Sohn, S.K. Kang, S.I. Woo, J. Mol. Catal. A: Chem. 186 (2002) 135–144.
[4] G. Pecchi, P. Reyes, I. Concha, J.L.G. Fierro, J. Catal. 179 (1998) 309–314.
[5] R. Prasad, L.A. Kennedy, E. Ruckenstein, Catal. Rev. Sci. Eng. 26 (1984) 1–58.

[6] L.F. Liotta, G. Di Carlo, G. Pantaleo, G. Deganello, Catal. Commun. 6 (2005) 329–336.
[7] C. Bozo, N. Guilhaume, E. Garbowski, M. Primet, Catal. Today 59 (2000) 33–45.
[8] D. Terribile, A. Trovarelli, C. de Leitenburg, A. Primavera, G. Dolcetti, Catal. Today 47 (1999) 133–140.
[9] T. Tian, M. Zhan, W. Wang, C. Chen, Catal. Commun. 10 (2009) 513–517.
[10] M. Alifanti, R. Auer, J. Kirchnerova, F. Thyrion, P. Grange, B. Delmon, Appl. Catal. B: Environ. 41 (2003) 71–81.
[11] H. Arai, M. Machida, Appl. Catal. A: Gen. 138 (1996) 161–176.
[12] F. Yin, S. Ji, P. Wu, F. Zhao, C. Li, J. Mol. Catal. A: Chem. 294 (2008) 27–36.
[13] M. Machida, K. Eguchi, H. Arai, J. Catal. 120 (1989) 377–386.
[14] M. Machida, K. Eguchi, H. Arai, J. Catal. 123 (1990) 477–485.

[15] B.W.L. Jang, R.M. Nelson, J.J. Spivey, M. Ocal, R. Oukaci, G. Marcelin, Catal. Today 47 (1999) 103–113.
[16] S. Reddy, S. Vyas, Energy Procedia 1 (2009) 149–154.
[17] K.S. Hui, C.Y.H. Chao, C.W. Kwong, M.P. Wan, Combust. Flame 153 (2008) 119–129.
[18] E. Pocoroba, E. Magnus Johansson, S.G. Järås, Catal. Today 59 (2000) 179–189.
[19] J. Zheng, X. Ren, Y. Song, X. Ge, React. Kinet. Catal. Lett. 97 (2009) 109–114.
[20] S. Li, X. Wang, J. Alloys Compd. 432 (2007) 333–337.
[21] S. Li, H. Liu, L. Yan, X. Wang, Catal. Commun. 8 (2007) 237–240.
[22] S. Cimino, A. Di Benedetto, R. Pirone, G. Russo, Catal. Today 83 (2003) 33–43.
[23] S. Eriksson, M. Boutonnet, S. Järås, Appl. Catal. A: Gen. 312 (2006) 95–101.